On Cavitation Aggressiveness and Cavitation Erosion on Marine Propellers using a URANS Method

[1,2]Themistoklis Melissaris*; [1]Norbert Bulten; [2,3]Tom van Terwisga;

[1]Wärtsilä Netherlands B.V., Drunen, The Netherlands; [2]Delft University of Technology, Delft, The Netherlands; [3]Maritime Research Institute (MARIN), Wageningen, The Netherlands

Abstract

Cavitation occurrence on the propeller blades may have severe effects, such as cavitation noise, vibrations in the aft ship, and material damage on propellers or rudder. While noise and vibrations affect comfort and stability, cavitation erosion might lead to a significant reduction of the propeller efficiency and structural integrity. Cavitation erosion prediction is therefore extremely important. However, it still remains a challenging issue, especially on marine propeller applications where computational time limit in a practical propeller design environment is imperative. This paper focuses on cavitation aggressiveness on the propeller blades of the KCD-193 model propeller. Cavitation intensity is assessed by the potential power density. Following the idea that the potential power is the basis of the cavitation aggressiveness, we found that by computing the potential power of the first layer of cells, in contact with the blade surface, it gives a useful first estimate of the regions that are exposed to a high erosion risk. The use of a mean field pressure, which is the time average of the local pressure, as the driving pressure behind the cavity collapse, was necessary to get a good match with experimental observations.

Keywords: Cavitation aggressiveness; model propeller; potential power; driving pressure.

Introduction

Cavitation erosion strongly impacts the efficiency and structural integrity of marine propellers. Although much is known about bubble dynamics and the material response, the problem of predicting cavitation damage remains unresolved. Nevertheless, the development of numerical flow simulations seems to offer a good prospect for predicting cavitation and cavitation erosion using computational methods. As propeller design applications require reliable results in acceptable timespan, any numerical method for turbulence modelling other than unsteady RANS is currently considered as too time consuming.

This study is based on the assumption that the collapse of vapor cavities is characterized by potential energy E_{pot}, related to the pressure gradient and the cavity volume [1-4]. During the collapse, this potential energy converts mainly into acoustic energy, which is transmitted to the surface, causing an impact on the wall. The magnitude of the impact depends on the distance between the center of the collapse and the surface, as well as on the direction of the acoustic wave towards the surface wall [9]. Moreover, the water quality and the gas content within the vapor cloud before the collapse, also influence the collapse dynamics and the propagation of the acoustic energy [10].

The process to calculate the contribution of each collapse to the surface, including all the aforementioned parameters, can be very time consuming, resulting in a large computational time. To this end, as a first step, only the contribution of the first layer of cells in contact with the blade surface is taken into account. As driving pressure, the time average of the local pressure in every cell is computed and used in the definition of the potential energy. It was found that using this mean field pressure, instead of the direct local pressure, gives results that agree well with the experiments.

Numerical Modeling

The equations solved are the Reynolds Averaged Navier-Stokes (RANS) equations. An incompressible segregated flow model is selected solving the integral conservation equations of mass and momentum in a sequential manner combined with the SIMPLE pressure-velocity coupling algorithm. A Eulerian multiphase model is used, treating the fluid as a single continuum, assuming a no-slip condition between liquid and vapor phase, with varying properties in space according to its composition. The volume fraction of the components is determined from the condition $a_v + a_l = 1$ while density and viscosity are defined as $\rho = a_l\rho_l + \alpha_v\rho_v$ and $\mu = a_l\mu_l + a_v\mu_v$ respectively.

The turbulence model used in this study is the k-ω SST turbulence model developed by Menter [5]. An empirical reduction of turbulence dissipative terms in two-phase regions has been applied, by modifying turbulent viscosity:

*Corresponding Author, Themistoklis Melissaris: themis.melissaris@wartsila.com

$$\mu_t = f(\rho) C_\omega \frac{k}{\omega}; \quad f(\rho) = \rho_v + \frac{(\rho_m - \rho_v)^n}{(\rho_l - \rho_v)^{n-1}}; \quad n \gg 1 \tag{1}$$

where ρ_v is the vapor density, ρ_l the liquid density and ρ_m the mixture density. For the constant n, a recommended value $n = 10$ has been used. This empirical modification improves the artificial increase of dissipation, generated by the no-slip condition between the two phases. The arbitrary reduction of the turbulent viscosity in the two face regions allows stronger shear flows, while dissipation in the pure liquid remains the same [6].

The cavitation model used is the model proposed by Schnerr-Sauer [7] based on a simplified Rayleigh-Plesset equation, which neglects the influence of bubble growth acceleration, as well as viscous and surface tension effects.

Erosion Modeling

Cavitation intensity is addressed by monitoring the initial potential power of the vapor structures. According to the approach proposed by [2], a vapor cloud contains potential energy which can be defined as follows:

$$E_{pot} = \Delta p \cdot V_{vap} \tag{2}$$

where $\Delta p = (p_\infty - p_{vap})$ is the difference between the surrounding pressure P_∞ and the vapor pressure P_{vap} and the vapor volume V_{vap}. Then, the potential power within the structure can be calculated as the time derivative of the potential energy

$$P_{pot} = \Delta p \cdot \frac{dV_{vap}}{dt} + \frac{dp}{dt} \cdot V_{vap} \tag{3}$$

and a potential power density can be estimated from:

$$\frac{P_{pot}}{V_{cell}} = \Delta p \cdot \frac{da}{dt} + \frac{dp}{dt} \cdot a \tag{4}$$

where $a = V_{vap}/V_{cell}$. To evaluate the cavitation aggressiveness on the surface, the contribution of every vapor structure should be taken into account. The transmitted energy on the surface, due to the collapse of a vapor cloud, depends on several factors, such as the distance of the cloud from the wall and the angle with which the emitted pressure wave hits the surface, the amount of dissolved gas within the initial bubbly cloud, and the water quality [9, 10]. The final erosion damage depends also on the material properties and on the material response to the pressure wave impact. In this study, we focus first on the evaluation of the cavitation intensity, considering only the vapor content of the cells in contact with the blade surface, and we neglect any collapse event away from the surface. The contributions of both time derivatives to the potential power density are computed separately, and compared with each other.

Another important element for the assessment of the cavitation intensity is the driving pressure P_∞ occurring in the Δp term of eq. 3. The driving pressure should describe the flow characteristics while being independent of the cavitation dynamics. The local instantaneous pressure is strongly influenced by the cavitation dynamics. Therefore, the time average of this local pressure is considered as the driving pressure. In this way, we neglect the high pressure peaks due to bubble collapses.

Case Description

The case used in this study is the King's College-D (KCD)-193 model propeller. This propeller has been tested at the Emerson Cavitation Tunnel (ECT) of Newcastle University [8]. Erosion tests and performance measurements in cavitating flow have been conducted. A 2D wake screen was used, located 0.4572 m from the propeller center, to simulate the wake field of the propeller. Figure 1 shows the propeller geometry within the computational domain, and the velocity distribution right before the propeller. The tunnel and propeller geometry, and the inlet boundary condition were provided by University of Strathclyde, Glasgow. Table 1 gives the propeller characteristics. The propeller was tested in two cavitating conditions, one in atmospheric and one in vacuum condition (see Table 2). The cavitation number is defined as

*Corresponding Author, Themistoklis Melissaris: themis.melissaris@wartsila.com

$$\sigma = \frac{P_{ref} - P_v}{0.5\rho\,(nD)^2} \tag{2}$$

where P_{ref} is the reference pressure, P_v the vapor pressure, ρ the liquid density, n the rotational speed and D the propeller diameter.

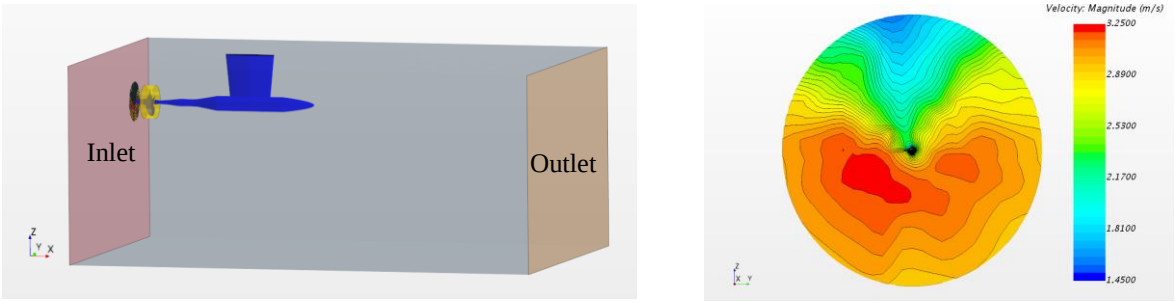

Figure 1. Computational domain (left) and the velocity distribution right before the propeller geometry (right).

Propeller Diameter	0.3048 m
P/D	1
Blade Area Ratio	0.65
Number of Blades	4

Table 1. Propeller Characteristics

Condition	P_{ref} (kPa)	n (RPM)	V_A (m/s)	J	σ
Atmospheric	116.72	1500	3	0.393	3.88
Vacuum	77.016	1500	3	0.392	2.52

Table 2. Conditions at which measurements were taken during the experiments.

For the grid generation, trimmed hexahedral cells were used with local refinements and prism layers along the wall, with such first cell distance so the average y+ value was well below 1 to resolve the viscous sublayer. An extra refinement was applied around the tip area to capture the tip vortex cavitation (Figure 2). After a sensitivity study, a grid with around 8.5 million cells was used, with 6 million cells at the rotating region. The rotation rate was 0.1 degrees per time step.

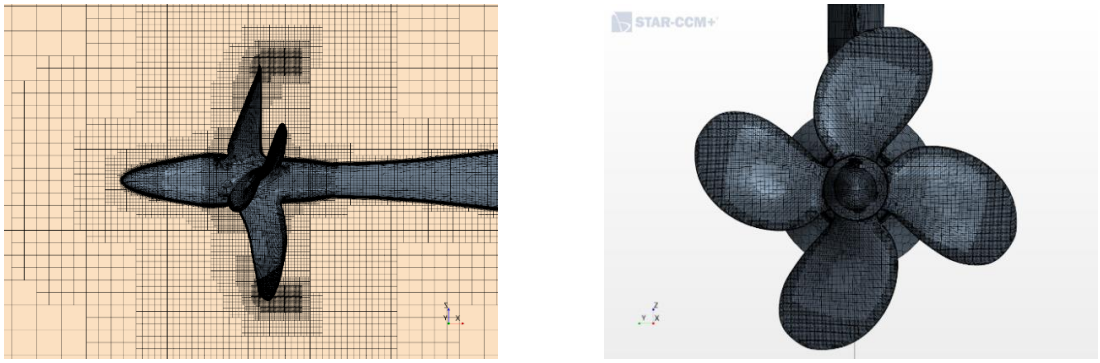

Figure 2. Computational grid. A refinement was used around the tip area to capture cavitation dynamics in detail.

Results

The propeller thrust and torque were calculated for both conditions (atmospheric and vacuum) and they were compared with experimental data. For the thrust, two values were computed, one including only the thrust of the propeller blades, and one including also the thrust and drag of the hub and the hubcap respectively. This was because the way the thrust coefficient was measured during the experiment is not known. The results are shown in Table 3. The uncertainties of the experiment are also unknown, and the presence of the wake screen, introduces an extra uncertainty in the numerical modelling. No uncertainty assessment was conducted for the computations in the current study, but we ensured compliance with existing Best Practice Guidlines. Following these guidelines and using previous studies on uncertainties we consider the discrepancy between the measurements and the CFD results as acceptable. The computed cavities showed a good qualitative agreement with the cavitation observations for both conditions. However, no quantitative comparison was possible as there is no experimental information regarding the total vapor volume. The

*Corresponding Author, Themistoklis Melissaris: themis.melissaris@wartsila.com

length of the tip vortex was slightly underestimated, but it is not of high importance in this case. Figure 3 and Figure 4 show the qualitative comparison.

		$K_{T_{Blades}}$	$K_{T_{Propeller}}$	$10K_Q$	Vapor Volume (m^3)
Atmospheric Condition	**Experiment**	0.374	0.374	0.541	-
	CFD	0.389	0.355	0.580	2.096E-05
	Difference %	4.14%	-5.18%	7.29%	-
Vacuum Condition	**Experiment**	0.371	0.371	0.554	-
	CFD	0.383	0.360	0.595	6.974E-05
	Difference %	3.14%	-2.95%	7.5%	-

Table 2. Thrust and torque coefficients and total vapor volume as computed with CFD for both atmospheric and vacuum conditions. K_T and K_Q are compared with the experimental measurements.

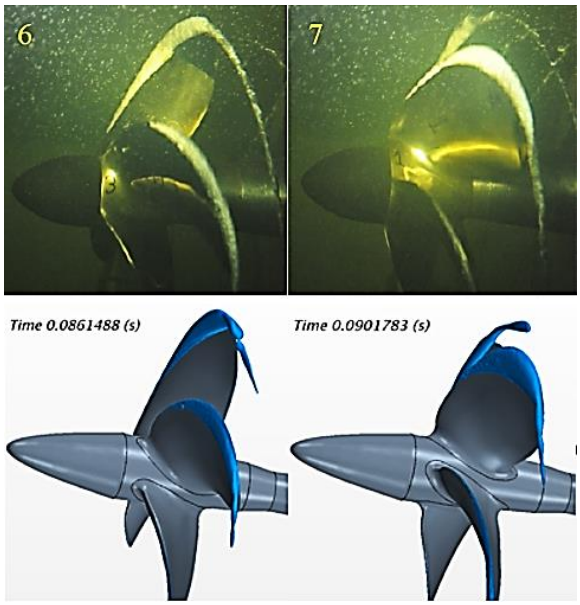

Figure 3. Qualitative comparison of the vapor volume between the experimental observations and the computations with iso-value of $a = 0.1$ in atmospheric condition [8].

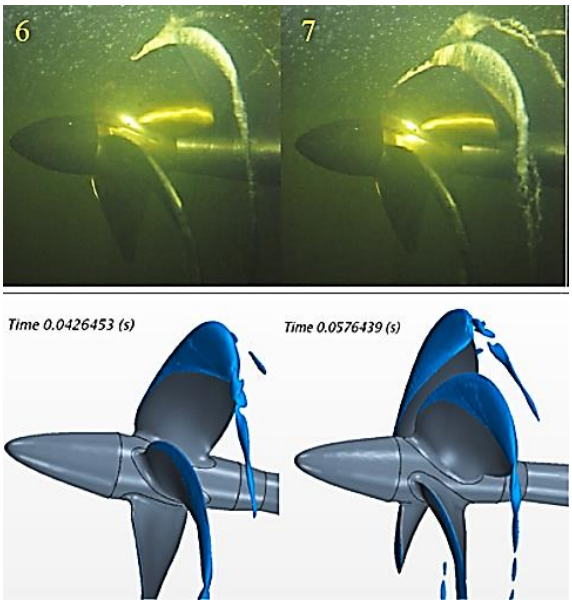

Figure 4. Qualitative comparison of the vapor volume between the experimental observations and the computations with iso-value of $a = 0.1$ for the vacuum condition [8]

The cavitation intensity on the propeller blades was estimated by calculating the potential power density during two propeller rotations. The statistical uncertainty of the total vapor volume was estimated to be around 0.5%. The two contributions to this power density (the relative variation of the vapor volume and the pressure) were computed. Two different interpretations for the driving pressure were used; the time average of the local pressure in every cell, in addition to the local instantaneous pressure. Not surprisingly, the results show that the time derivative of the void fraction (Figure 5a) contributes much more than the averaged pressure time derivative term (Figure 5b). This result is in line with Leclercq et. al. [8]. On the other hand, when the local instantaneous pressure would have been used for the computation of the two terms, either the cavitation intensity would be much lower (Figure 5c) or a high intensity would be located only at the leading edge (Figure 5d), which was not observed in the experiment [8].

Li et. al. [4] found that the variation of the local pressure in time showed higher contribution to the cavitation aggressiveness than the variation of the volume fraction, for two NACA hydrofoils. Their outcome agrees with our results with the local instantaneous pressure as the driving pressure behind the collapse (figure 5c and 5d). However the high intensity areas in our case do not agree with the experiments. On the other hand, using the mean local pressure as the driving pressure, shows a higher contribution of the vapor volume variation to the cavitation aggressiveness. In addition to that, the results agree well with the paint test (Figure 6), showing the importance of a correct definition of the driving pressure when assessing the erosion intensity.

*Corresponding Author, Themistoklis Melissaris: themis.melissaris@wartsila.com

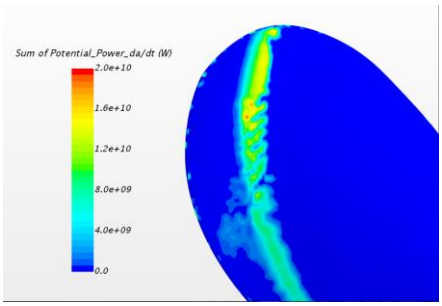

Figure 5a. The sum of $\Delta p \cdot \frac{da}{dt}$ on the blade surface after two rotations, with the time averaged local pressure for p_∞ in Δp.

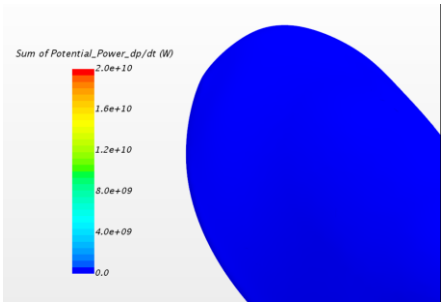

Figure 5b. The sum of $\frac{dp}{dt} \cdot a$ on the blade surface after two rotations, with the time averaged local pressure for p_∞ in Δp.

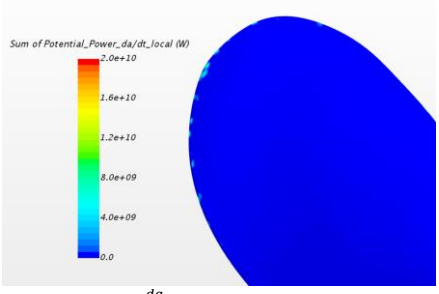

Figure 5c. The sum of $\Delta p \cdot \frac{da}{dt}$ on the blade surface after two rotations, with the local instantaneous pressure for p_∞ in Δp.

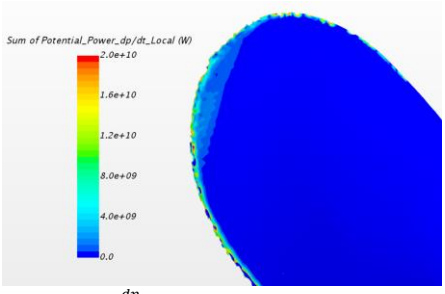

Figure 5d. The sum of $\frac{dp}{dt} \cdot a$ on the blade surface after two rotations, with the local instantaneous pressure for p_∞ in Δp.

Figure 6, compares the computed cavitation aggressiveness on the propeller blades with the paint erosion tests, for atmospheric (Figure 6a and 6b) and vacuum condition (Figure 6c and 6d). There is a fair qualitative agreement between the experimental damage location and the computed region of high erosion risk indicated by the increased potential power density. Nevertheless, this can only be a first indication of the areas with high erosion risk, because only the first layer of cells, connected with the surface, have been taken into account.

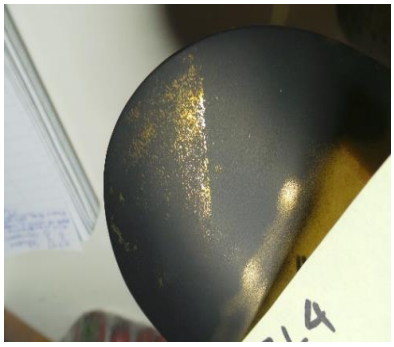

Figure 6a. Experimental erosion observation in atmospheric condition [8].

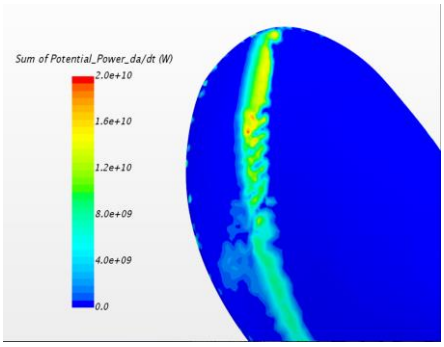

Figure 6b. Computed potential power after two propeller rotations in atmospheric condition.

Figure 6c. Experimental erosion observation in vacuum condition [8].

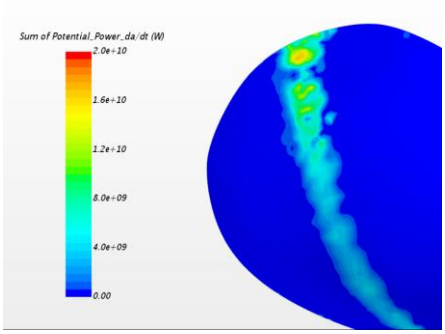

Figure 6d. Computed potential power after two propeller rotations in vacuum condition.

*Corresponding Author, Themistoklis Melissaris: themis.melissaris@wartsila.com

Additional contribution should be accounted for all the structures close to the surface, by considering the distance and the direction of the collapse towards the surface. Moreover, the impact of the water quality and the bubble gas content has also been neglected. Finally, the material response should be taken into account as well, to be able to calculate the actual damage and material loss on the propeller blades.

Conclusion

Cavitation erosion can cause severe damage to the propeller blades, and gives opposite design trends to fuel efficiency, rendering cavitation erosion risk assessment imperative, already in the design stage. Making an early stage propeller erosion assessment requires the right selection of an erosion model (physical modelling), in addition to the numerical modelling. In this study, the energy balance approach has been adopted [2, 10], to estimate cavitation intensity. The contribution of both the vapor volume and pressure derivative terms to the potential power density has been evaluated. In every cell, the time average of the local pressure was used as the driving pressure p_∞, and we compared the results with the results based on the local instantaneous pressure. As a first step, only the first layer of cells, connected with the surface were considered, to facilitate the erosion intensity assessment. We found that the areas with high potential power density agree well with the erosion observations for both atmospheric and vacuum condition, when the mean field pressure is used. However, the contribution of all the vapor structures in the domain should also be considered, to get a representative estimate of the cavitation erosion risks. If, furthermore, an estimate of the damage would be needed, the material response would have to be invoked, in order to compute the material loss on the propeller surface. This will be further investigated in the future. We conclude that this method can be used for an initial and quick evaluation of the high erosion risk areas on the propeller blades, useful for propeller design optimization. Further studies are planned to evaluate applicability of this erosion criterion for propeller optimization in behind conditions.

Acknowledgements

The kind cooperation of Strathclyde University by making their erosion propeller data available to our computational study is highly appreciated and acknowledged.

References

[1] Hammit, F. G., (1963). *Obserbations on Cavitation Damage in a Flowing System*. ASME J. Basic Engineering, **85** (3), p. 347-359.

[2] Fortes-Patella, R., and Reboud, J. L., (1998). *A New Aproach to Evaluate the Cavitation Erosion Power*. ASME Journal of Fluids Engineering, vol 120, p. 335-344.

[3] Bark, G., Berchiche, N., and Grekula, M., (2004), *Application of Principles for Observation and Analysis of Eroding Cavitation-The EROCAV Observation Handbook*, 3.1 ed., Chalmers University of Technology, Goteborg, Sweden.

[4] Li, Z., and Terwisga, T. J. C. (2014), *Assessment of Cavitation Erosion with a URANS Method*. ASME J. Fluids Eng., 136, p. 041101-1.

[5] Menter F., (1994). *Two-equation eddy-viscosity turbulence modeling for engineering applications*. AIAA Journal, vol. 32, p. 1598-1605.

[6] Reboud J.-L, Stutz, B., and Coutier, O., (1998). *Two-phase flow structure of cavitation: experiment and modelling of unsteady effects*, in Third International Symposium on Cavitation, Grenoble, France.

[7] Sauer J., (2000). "*Instationär kavitierende strömungen - Ein neues modell, basierend auf fron capturing (VoF) und blasendynamik*" Ph.D. Thesis, Karlsruhe University, Karlsruhe, Germany.

[8] Mantzaris, A., Aktas, B., Fitzsimmons, P., .and Atlar, M., (2015). "*Establishment and verification of reproducible method for coating propeller blades for erosive cavitation detection*", Forth International Conference on Advance Model Measurement Technologies for the Maritime Industry, Istanbul, Turkey

[9] Leclercq, C., Archer, A., and Fortes-Patella, R., (2016). *Numerical investigations on cavitation intensity for 3D homogeneous unsteady viscous flows*, IOP Conference Series: Earth and Environmental Science, 49(9), p. 092007, IOP Publishing

[10] Fortes-Patella, R., Challier, G., Reboud, J. L., .and Archer, A., (2013), "*Energy Balance in Cavitation Erosion: From Bubble Collapse to Indentation of Material Surface*", ASME J. Fluids Eng., 135, p. 011303-1.

[11] Usta, O., Aktas, B., Maasch, M., Turan, O., Atlar, M., and Korkut, E., (2017), "*A study on the numerical prediction of cavitation erosion for propellers*", Fifth International Symposium on Marine Propulsion, Espoo, Finland.

*Corresponding Author, Themistoklis Melissaris: themis.melissaris@wartsila.com